Theoretical Analysis of the Electronic Spectra of Benzaldehyde

Vicent Molina† and Manuela Merchán*

Departamento de Química Física, Universitat de València, Dr. Moliner 50, Burjassot, E-46100 Valencia, Spain

Received: October 31, 2000; In Final Form: February 1, 2001

The electronic spectrum of benzaldehyde has been studied by using multiconfigurational second-order perturbation theory through the multistate extension (MS-CASPT2). The $n\pi^*$ $1^1A''$ state, placed vertically at 3.71 eV, is assigned to the lowest band. The $1^1A' \rightarrow 2^1A'$ and $1^1A' \rightarrow 3^1A'$ transitions, of $\pi\pi^*$ nature, located at 4.33 and 4.89 eV, are responsible for the second- and third-energy bands, respectively. The most intense feature involves the $4^1A'$ and $5^1A'$ $\pi\pi^*$ excited states, calculated to be 5.98 and 6.23 eV above the ground state. In addition, excited states corresponding to the low-lying Rydberg series are related to the available experimental data. Geometry optimizations for the ground state and low-lying excited states of both $n\pi^*$ and $\pi\pi^*$ characters have been carried out at the CASSCF level. The relative ordering of the lowest $n\pi^*$ and $\pi\pi^*$ triplet states varies depending on the geometry employed. Furthermore, the $S_1(n\pi^*)$ and $T_2(\pi\pi^*)$ potential hypersurfaces are found to intersect upon relaxation in S_1, providing a possible explanation for the efficient singlet−triplet intersystem crossing occurring in benzaldehyde.

1. Introduction

Within an on going project dealing with the theoretical characterization of the electronic spectra of monosubstituted benzenes, we have recently analyzed the low-lying excited states of styrene, the simplest aryl olefin.[1,2] Presented in this paper are the results from a parallel investigation carried out on benzaldehyde, the simplest aromatic carbonyl compound which is isoelectronic to styrene. To the best of our knowledge, there are no high-level ab initio results available on benzaldehyde. We believe that the results here reported can yield new light on the interesting and complex photochemistry of the system.

The spectroscopy of benzaldehyde has been extensively studied experimentally. An excellent review of its vapor phase spectroscopy can be found in the 1996 paper of Silva and Reilly.[3] As might be expected, the electronic spectra of benzaldehyde and styrene are quite similar, except for the presence of an $n\pi^*$ state in the former. The vacuum ultraviolet spectra of benzaldehyde are known since long ago.[4−6] Four bands have been recorded in the low-energy region of the one-photon electronic spectrum in increasing order of intensities and excitation energies. The benzaldehyde $S_0 \rightarrow S_1(n\pi^*)$ weak band shows a well-resolved structure in the room-temperature vapor spectrum. The most intense feature of this band at 3.34 eV has been established as the origin.[7,8] The remaining bands are assumed to be of $\pi\pi^*$ character. The maximum of the second-energy band appears at 4.51 eV with an oscillator strength of 0.02. The maximum of the third-energy band is located at 5.34 eV with an oscillator strength of 0.26. The fourth band of the absorption spectrum corresponds to a broad and intense system with a maximum around 6.36 eV and a total oscillator strength value for the overlapped bands of 1.7.[6] After excitation to the $S_2(\pi\pi^*)$ state, benzaldehyde is decomposed into benzene and carbon monoxide.[9] The $S_0 \rightarrow S_2$ band origin has been observed at 4.36 eV in the jet-cooled spectrum.[3] The third-energy band has been investigated under jet-cooled conditions as well.[10] The strongest absorption band system with its maximum around 6.4 eV has not been investigated in detail. Whether its intensity comes mainly from one or several electronic transitions still needs to be clarified.

Benzaldehyde, like other aromatic carbonyl compounds, exhibits strong phosphorescence in the gas phase and has been used as a triplet energy donor (see, e.g., Berger et al.[9]). However, the triplet manifold has not been as well characterized as the singlet. Only the $n\pi^*$ triplet state has been measured in the gas phase. Great efforts have been devoted to determine the location of the lowest $\pi\pi^*$ triplet state relative to the lowest $n\pi^*$ triplet state.[9,11−13] The relative location depends on the environment and solvent perturbation.[14] The band origin of $T_1(n\pi^*)$ has been measured at 3.12 eV from the phosphorescence excitation spectrum of isolated benzaldehyde in $S_0 \rightarrow T$ region, below the S_1 origin.[11] It is consistent with the corresponding band origin observed in the phosphorescence spectrum.[15,16] Experimental evidence also gives support to the presence of a second triplet state, possibly of $\pi\pi^*$ character, somewhat above $T_1(n\pi^*)$ but close to it. As discussed below, it is confirmed by the present results.

Despite the importance of the system, only a few theoretical studies have been previously performed on benzaldehyde. The vertical excitation energies have been computed at the semiempirical level[6,17,18] and the adiabatic transitions at the CIS level.[3] The current study includes electron correlation effects, from first principles, using the multiconfigurational second-order perturbation theory CASPT2,[19,20] taking into account the indirect interaction of the states within the framework of the multistate CASPT2 (MS-CASPT2) algorithm.[21] The successful performance of the CASPT2 method in computing differential correlation effects for excitation energies has been illustrated in a number of earlier applications.[22−24] The MS-CASPT2 results for both vertical and nonvertical electronic transitions provide a more complete picture for a better understanding of the spectroscopic behavior of benzaldehyde on theoretical grounds and make possible confident assignments. They serve

* To whom correspondence should be addressed. E-mail: Manuela.Merchan@uv.es. Phone: Int + 34−96−398−3155. Fax: Int + 34-96-398-3156.

† E-mail: Vincent.Molina@uv.es.

10.1021/jp004041t CCC: $20.00
Published on Web 03/22/2001

TABLE 1: Details of the CASSCF Wave Functions Employed for the Computation of the Considered Valence and Rydberg Excited States of Benzaldehyde.

state	orbitals a′ [a]	orbitals a″ [b]	no. electrons [c]	no conf. [d]	N_{states}[e]
^{1}A′($\pi\pi$*)	0	8	8	1764	8
^{3}A′($\pi\pi$*)	0	8	8	2352	1
^{1}A″(n → π^*)	1	8	10	2352	1
^{3}A″(n → π^*)	1	8	10	3696	1
^{1}A′(π → 3p$_z$, 3d$_{xz}$, 3d$_{yz}$)	0	11	8	32 670	10
^{1}A″(n → 3p$_z$, 3d$_{xz}$, 3d$_{yz}$)	1	11	10	76 230	6
^{1}A″(π → 3s, 3p$_x$, 3p$_y$, 3d$_{xy}$, 3d$_{x^2-y^2}$, 3d$_{z^2}$)	9	4	4	1140	9
^{1}A′(n → 3s, 3p$_x$, 3p$_y$, 3d$_{xy}$, 3d$_{x^2-y^2}$, 3d$_{z^2}$)	10	4	6	20 925	9

[a] Number of active orbitals of a′ symmetry. [b] Number of active orbitals of a″ symmetry. [c] Number of active electrons. [d] Number of configurations in the CASSCF wave functions. [e] States included in the average CASSCF calculations.

both to complement the earlier studies and to bring a firm foundation for a theoretical elucidation of the photochemistry of benzaldehyde. Two main issues have been addressed. How many electronic transitions are responsible for each of the observed absorption bands, and key to characterize the triplet manifold, what about the relative location of the two lowest triplet states?

The paper is organized as follows. Computational details are described in the next section. After that, the equilibrium geometries of the ground and low-lying excited states are presented. Results and analysis on the computed singlet−singlet and singlet−triplet absorption spectra and 0−0 transitions are subsequently considered, together with comparisons to previous findings. Our conclusions and answers to the questions arising from the discussion above are summarized in the last section.

2. Methods and Computational Details

Generally contracted basis sets of atomic natural orbital (ANO) type obtained from the C,O(14s9p4d)/H(8s) primitive sets[25] with the C,O[3s2p1d]/H[2s] contraction scheme were used. These basis sets were designed to treat correlation and polarization effects optimally. They were supplemented with two s-, two p-, and two d-type diffuse functions placed at the charge centroid of the cation. The exponents can be found elsewhere.[26] The efficiency of the basis set has been illustrated in a number of earlier studies of organic compounds performed with the same methods (biphenyl,[27] stilbene,[28,29] styrene,[1,2] 1-phenylpyrrole,[30] etc.).

The reference wave functions and the molecular orbitals were obtained from average CASSCF calculations, including all of the states of interest for a given symmetry. Details on the active spaces employed, together with the number of configurations involved in the CASSCF wave functions, and type of states computed are given in Table 1. For the excited states of $\pi\pi$* character, the active space comprises the valence π molecular orbitals and the π electrons. For the computation of the excited states involving the lone pair orbital localized on the oxygen atom, the active space was enlarged accordingly. In addition, those active spaces were extended to include Rydberg orbitals as appropriate. For Rydberg states that the Rydberg orbital belongs to the irreducible representation a′ of the C_s point group, only four π orbitals were kept in the active space (with four π electrons).

The CASSCF wave functions were employed as reference functions in a single-state second-order perturbation CASPT2 treatment.[19,20] The coupling of the CASSCF wave functions via dynamic correlation was dealt with by means of the extended multi-state CASPT2 approach, the MS-CASPT2 method.[21] An effective Hamiltonian matrix is constructed where the diagonal elements correspond to the CASPT2 energies and the off-diagonal elements introduce the coupling to second order in the dynamic correlation energy. In this manner, the states considered in a MS-CASPT2 computation can be treated simultaneously with the correlation effects on the reference functions included, and the possibly erroneous valence−Rydberg mixing can be removed.

Perturbation modified CAS (PMCAS-CI) reference functions (the model states),[21] i.e., linear combinations of all CAS states involved in the MS-CASPT2 calculation, were employed to compute the corresponding transition dipole moments according to the CASSI protocol.[31,32]

All calculations were carried out using the MOLCAS-4 quantum-chemical package.[33]

TABLE 2: Equilibrium Geometries for the Ground and Low-lying $\pi\pi$* and $n\pi$* Singlet and Triplet Excited States Optimized at the CASSCF Level Employing the ANO C,O[3s2p1d]/H[2s] Basis Set.

parameter[a]	1^{1}A′(GS)	1^{3}A″	1^{3}A′	1^{1}A″	2^{1}A′
r(C$_1$O)	1.204[b]	1.343	1.231	1.354	1.214
r(C$_1$C$_2$)	1.485	1.406	1.427	1.395	1.455
r(C$_2$C$_3$)	1.403	1.423	1.485	1.429	1.438
r(C$_2$C$_4$)	1.397	1.425	1.469	1.431	1.442
r(C$_3$C$_5$)	1.393	1.390	1.362	1.388	1.437
r(C$_4$C$_6$)	1.399	1.386	1.358	1.384	1.433
r(C$_5$C$_7$)	1.402	1.403	1.444	1.405	1.428
r(C$_6$C$_7$)	1.395	1.406	1.465	1.409	1.427
r(C$_1$H$_1$)	1.100	1.081	1.096	1.081	1.099
∠(C$_2$C$_1$O)	124.6	122.4	123.7	122.5	124.4
∠(C$_1$C$_2$C$_3$)	121.0	122.0	121.2	122.1	121.3
∠(C$_2$C$_1$H$_1$)	115.5	124.6	117.0	124.5	115.8

[a] Bond distances in angstroms and angles in degrees (see Figure 1 for atom numbering). [b] CASPT2 optimized bond distance, 1.232 Å.

3. Results and Discussion

As a preliminary step toward the theoretical understanding of the electronic spectrum of benzaldehyde, the geometry for the ground state and low-lying singlet and triplet excited states are first considered. The properties of the excited states vertically computed are next analyzed. After that, the relative location of the excited states at different zones of the hypersurface together with the nonvertical transition energies are discussed. Furthermore, the present findings will be compared with previous theoretical results and available experimental data.

3.1. Equilibrium Structures. Geometry optimizations for the ground state and low-lying excited states of both $n\pi$* and $\pi\pi$* characters were carried out at the π-CASSCF level. For the $n\pi$* excited states, the active space was enlarged with the oxygen lone pair. In both cases, the ANO C,O[3s2p1d]/H[2s] basis set was employed. The optimized geometric parameters for the singlet and triplet excited states are listed in Table 2. All optimizations were constrained to C_s symmetry, with the symmetry plane being the molecular plane. The atom numbering scheme used throughout this study is defined in Figure 1.

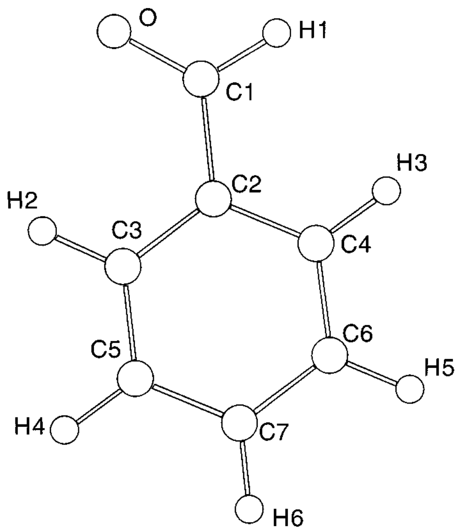

Figure 1. Atom labeling of the benzaldehyde molecule.

In the ground state, the ring is computed to have a mean carbon−carbon distance of 1.398 Å, close to the experimental datum (1.395 Å).[34] The trends are similar as those found in styrene.[1] The π electron correlation included at the π-CASSCF level, which tends to overestimate bond lengths, is partially compensated by the lack of σ electron correlation. However, because it is known that the carbonyl bond distance strongly depends on the level of correlation,[35−37] the C=O bond length for the ground state has been optimized at the π-CASPT2 level by using a pointwise procedure. It has been subsequently employed in the computation of the excitation energies. The π-CASPT2 result, 1.232 Å, is close to the MP2 result (1.231 Å) computed with the same basis set. The optimized bond distance at the π-CASSCF level, 1.204 Å, although consistent with the corresponding experimental datum for formaldehyde (1.210 Å[38]), is underestimated with respect to the CASPT2 (MP2) result. Compared to the electron diffraction datum for benzaldehyde (1.212 Å), the π-CASSCF result is underestimated by 0.008 Å. In contrast, the CASPT2 finding leads to a too long bond distance, overestimated by 0.020 Å. A planar conformation is expected, which is also supported by microwave rotational experiments (see discussion in the 1996 paper by Silva and Reilly[3] and references therein).

The mean ring carbon−carbon bond lengths in $S_1(n\pi^*)$ and $T_1(n\pi^*)$ are similar, 1.406 and 1.408 Å, respectively. They are somewhat increased with respect to the ground state (≈0.01 Å). Consistent with the nature of the states, the C=O bond length is clearly elongated for both singlet and triplet $n\pi^*$ excited states.

The mean ring carbon−carbon bond distances for the $1^3A'$ and $2^1A'$ are 1.431 and 1.434 Å, respectively. The geometric changes of the $2^1A'$ excited state, with respect to the ground state, reflect the localized nature of the $1^1A' \rightarrow 2^1A'$ electronic transition in the aromatic part of the molecule. The $\pi\pi^*$ triplet excited-state develops a clear quinoid character with shorter C_1C_2, C_3C_5, and C_4C_6 bond distances than in the ground state. Similar trends have also been found in the respective excited states of styrene.[1] The geometrical parameters computed at the CIS level[3] are underestimated with respect to the π-CASSCF results. Nevertheless, the trends obtained in both cases are consistent except for the $S(\pi\pi^*)$ state ($2^1A'$). It seems to point out to the different nature of the singlet excited state computed by Silva and Reilly,[3] which resembles to the $T(\pi\pi^*)$ state, described mainly by one-electron promotion from the highest occupied molecular orbital (HOMO) to the lowest unoccupied molecular orbital (LUMO). It is not surprising considering that the CIS method[39] places the two lowest vertical $\pi\pi^*$ singlet excited states nearly degenerate. As discussed below, the HOMO → LUMO singlet excited state is not the lowest in the singlet manifold. A mapping of the lowest $n\pi^*$ and $\pi\pi^*$ states of benzaldehyde at their respective optimized geometries has also been carried out. The results are listed in Table 3 and shall be discussed below as appropriate.

TABLE 3. Mapping of the Lowest nπ^* and $\pi\pi^*$ States of Benzaldehyde at the CASPT2 Level Employing the Optimal Geometries for the $1^1A'$(GS), $1^3A''(n\pi^*)$, $1^3A'(\pi\pi^*)$, $1^1A''(n\pi^*)$, and $2^1A'(\pi\pi^*)$ States[a]

state	optimized geometries for the states				
	$1^1A'$	$1^3A''$	$1^3A'$	$1^1A''$	$2^1A'$
$1^1A'$	0.00	0.48	0.37	0.57	0.10
$1^3A''$	3.40	3.07	3.52	3.07	3.49
$1^3A'$	3.49	3.40	3.16	3.39	3.32
$1^1A''$	3.71	3.29	3.76	3.27	3.78
$2^1A'$	4.33	4.42	4.42	4.46	4.00

[a] The diagonal terms correspond to the adiabatic electronic transitions.

3.2. Vertical Spectra of Benzaldehyde. The computed vertical excitation energies at the PMCAS-CI and MS-CASPT2 levels of theory, together with oscillator strengths of the corresponding transitions, and selected experimental data are compiled in Table 4. Figure 2 shows schematically the π valence molecular orbitals for benzaldehyde and styrene with their respective canonical orbital energies, obtained at the Hartree−Fock level with the C,O[3s2p1d]/H[2s] basis set.

3.2.1. Valence Singlet Excited States. At the highest level of theory employed, five valence singlet excited states occur below the lowest Rydberg transition. These valence excited states are computed to lie within the energy range of 3.71−6.23 eV (MS-CASPT2 results). Strong electronic transitions involve three valence singlet excited states ($3^1A'$, $4^1A'$, and $5^1A'$). Computed at the PMCAS-CI level, corresponding electron density differences relative to the ground state and natural orbital plots for the low-lying valence $\pi\pi^*$ states are shown in Figures 3 and 4, respectively.

The lowest singlet excited state $1^1A''$ is calculated to lie vertically 3.71 eV above the ground state. It is the expected $1^1A''(n\pi^*)$ state. The computed excitation energy and small oscillator strength are consistent with the related dipole-forbidden feature obtained in formaldehyde (3.91 eV)[35] and acetone (4.18 eV).[36] From the electron density difference plot (cf. Figure 3), the local nature within the carbonyl group of the transition is easily inferred. The adiabatic transition to $1^1A''$ is calculated at 3.27 eV (see Table 3), in agreement with the experimental determination of the band origin at 3.34 eV.[11]

The lowest singlet excited state of $\pi\pi^*$ character ($2^1A'$) is computed at 4.33 eV. It corresponds to a weak transition. It can be related to the second-energy experimental band with the maximum recorded around 4.51 eV.[6] In terms of the natural orbitals of the PMCAS-CI wave function, the state can be mainly described by the one-electron promotion (HOMO − 1) → LUMO with some contribution of the HOMO → (LUMO + 1) (cf. Figure 4).

The $3^1A'$ state is dominated by the singly excited configuration HOMO → LUMO. The state is calculated to lie 4.89 eV above the ground state. Transition to the $3^1A'$ state, with a computed oscillator strength of 0.33, can be related to the observed third-energy band, with maxima at 5.34 eV in the gas phase[6] and 5.15 eV in the jet-cooled sample.[10] The computed

TABLE 4: Calculated Vertical Excitation Energies (in eV), Oscillator Strengths (*f*), and Dipole Moments (*μ* in Debyes) for Benzaldehyde[a]

state	PMCAS-CI	MS-CASPT2	f	μ	Exp. data ΔE	Exp. data f
			singlet states			
$1^1A'$(GS)				3.87		
$1^1A''$	3.86	3.71	$<10^{-3}$	1.23	3.34 (0−0)[b]	
$2^1A'$	4.75	4.33	0.002	4.44	4.51[c]	0.02[c]
$3^1A'$	7.05	4.89	0.331	6.07	5.34[c],5.15[d]	0.26[c]
$4^1A'$	8.06	5.98	0.396	4.66		
$5^1A'$	8.54	6.23	0.547	3.72	6.36[c]	1.7[c]
$2^1A''(\pi \rightarrow 3s)$	6.78	6.54	0.004	4.00		
$6^1A'(n \rightarrow 3s)$	6.48	7.03	0.004	8.30		
$7^1A'$	7.13	7.07	0.001	3.10		
$3^1A''(\pi \rightarrow 3p_y)$	7.26	7.18	0.004	1.31		
$4^1A''(\pi \rightarrow 3p_x)$	7.43	7.34	0.007	2.83		
$8^1A'(\pi \rightarrow 3p_z)$	6.77	7.50	0.013	1.79		
$9^1A'$	7.92	7.58	0.062	2.42		
$10^1A'(\pi' \rightarrow 3p_z)$	6.87	7.59	0.034	5.61		
$5^1A''(n \rightarrow 3p_z)$	8.03	7.67	$<10^{-3}$	1.83		
$11^1A'(\pi \rightarrow 3d_{yz})$	7.50	7.72	0.001	5.94		
$12^1A'(n \rightarrow 3p_y)$	7.03	7.77	0.022	7.75		
$13^1A'(\pi \rightarrow 3d_{yz})$	7.53	7.83	0.002	5.68		
$14^1A'$	8.15	7.88	0.015	1.69		
$6^1A''(\pi \rightarrow 3d_{x^2-y^2})$	7.91	7.95	$<10^{-3}$	4.39		
$7^1A''(\pi \rightarrow 3d_{xy})$	8.00	8.03	$<10^{-3}$	4.79		
$8^1A''(\pi \rightarrow 3d_{z^2})$	8.08	8.11	0.001	5.94		
$15^1A'(\pi \rightarrow 3d_{xz})$	7.43	8.14	0.003	5.98		
$9^1A''(n \rightarrow 3d_{xz})$	8.60	8.34	$<10^{-3}$	6.64		
$10^1A''(n \rightarrow 3d_{yz})$	8.63	8.38	$<10^{-3}$	2.55		
$16^1A'(n \rightarrow 3d_{x^2-y^2})$	7.60	8.39	0.009	4.64		
$17^1A'(\pi \rightarrow 3d_{xz})$	7.59	8.42	0.001	7.68		
$18^1A'(n \rightarrow 3d_{xy})$	7.63	8.44	0.005	8.05		
$19^1A'(n \rightarrow 3d_{z^2})$	7.78	8.57	0.022	6.10		
			triplet states			
$1^3A''$	3.62	3.40		1.14	3.12 (0−0)[b,e]	
$1^3A'$	3.58	3.49		3.23	3.3 (0−0)[f]	

[a] Experimental data are also included. [b] From sensitized phosphorescence excitation spectrum of jet-cooled benzaldehyde, Ohmori et al.[11] [c] Absorption spectrum in the vapor phase at room temperature, Kimura and Nagakura (1965).[6] [d] From direct absorption spectrum of jet-cooled benzaldehyde, Leopold et al. (1981).[10] [e] Origin of the phosphorescence spectrum, Koyanagi and Goodman (1979).[15] [f] Taken from Ridley and Zerner (1979).[18]

excitations energies for both styrene and benzaldehyde are somewhat below the observed band maxima. It seems to point out that, for the second $\pi\pi^*$ transition of these molecules, the absorption maxima does not correspond to the vertical transition. Indeed, a substantial sharpening of the vibronic structure occurs when the molecules are cooled in supersonic expansions, showing for benzaldehyde a very strong peak at 5.15 eV close to the 0−0 transition (5.12 eV).[10]

In the energy region of 6.0−6.2 eV, two electronic transitions are computed at 5.98 and 6.23 eV, with high predicted intensities, which can be related to the fourth-energy absorption band with a maximum around 6.4 eV in the vapor phase spectrum. The $4^1A'$ state is described mainly by the (HOMO) → (LUMO + 1) singly excited configuration with some contribution from the (HOMO − 1) → (LUMO) one-electron promotion. It is actually the corresponding plus linear combination involving the (HOMO − 1), HOMO, LUMO, and (LUMO + 1), whereas the $2^1A'$ state corresponds to the respective minus linear combination. The plus character of the $4^1A'$ state is in accordance with the corresponding relatively large oscillator strength (0.4). Transition to the $5^1A'$ state at 6.23 eV with an oscillator strength of 0.55 is predicted to be the most intense feature of the spectrum. The $5^1A'$ state is described mainly by the (HOMO − 1) → (LUMO + 1) singly excited configuration. In both styrene and benzaldehyde, the transition $1^1A' \rightarrow 5^1A'$ has the largest oscillator strength. The nature of the $5^1A'$ is similar in both systems.

The SCF orbital energies of the canonical π orbitals, calculated with the same basis set for both styrene and benzaldehyde (see Figure 2), can be used to rationalize the observed trends by assuming that the relative transition energies are related to orbital energy differences between the two molecules. In this manner, on the basis of similar orbital energy difference between the (LUMO + 1) and (HOMO − 1), 12.4 and 12.7 eV for styrene and benzaldehyde, respectively, the $1^1A' \rightarrow 5^1A'$ transition can be estimated to have a similar excitation energy, as it is actually the case (6.19 eV for styrene[1] vs 6.23 eV for benzaldehyde). The $4^1A'$ (5.98 eV) of benzaldehyde bears the same character as the $6^1A'$ (6.30 eV) of styrene (a plus state). In styrene, the orbital energy differences LUMO−(HOMO − 1) and (LUMO + 1)−HOMO have the same value, 11.5 eV. Therefore, they interact effectively in styrene yielding to a larger splitting between the corresponding minus and plus linear combinations. As a result, the plus state in styrene is pushed up about 0.3 eV with respect to benzaldehyde. The minus and plus states in benzaldehyde are mainly composed of the one-electron promotion (HOMO − 1) → LUMO and HOMO → (LUMO + 1), respectively. Because of the larger energy difference between LUMO−(HOMO − 1) (11.4 eV) and (LUMO + 1)−HOMO (12.6 eV), the resulting interaction is not so pronounced in benzaldehyde as it is in styrene. On the other hand, the $4^1A'$ of styrene computed at 6.08 eV,[1] with a doubly excited character predominantly, has its analogue in benzaldehyde at 7.07 eV ($7^1A'$, cf. Table 4). The largest

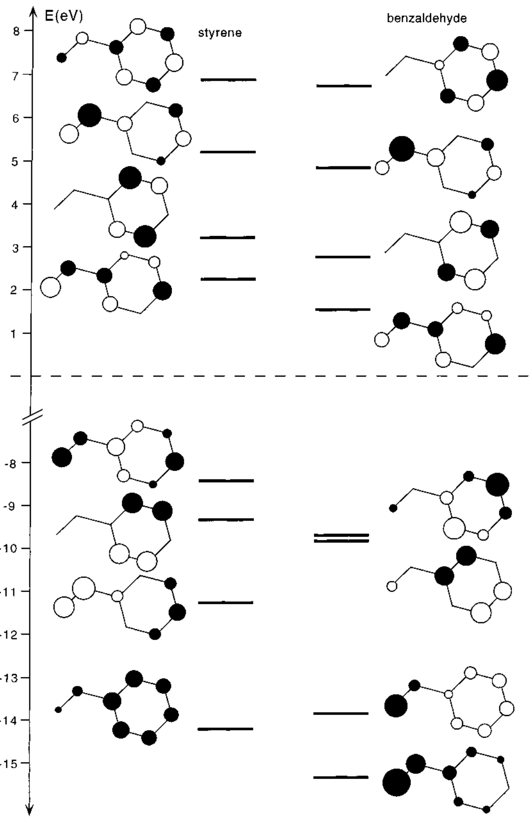

Figure 2. Qualitative diagram showing the highest four occupied and lowest four unoccupied π molecular orbital distribution of styrene and benzaldehyde. Orbital energies correspond to the canonical MOs using the ANO-type C,O[3s2p1d]/H[2s] basis set.

contribution in the wave function comes from the two-electron promotion (HOMO → LUMO)^2. Because the spacing between HOMO and LUMO is about 0.7 eV smaller in styrene than in benzaldehyde, the doubly excited state in the carbonyl compound is placed around 1 eV above that of the aromatic olefin.

In accordance with the nature of the excited states, the computed polarization directions for benzaldehyde are similar to those obtained for styrene, except for the lowest $\pi\pi^*$ transition. The $1^1A' \rightarrow 2^1A'$ transition is found to be polarized along the short and long inertial axis of benzaldehyde and styrene, respectively. Such a reverse polarization directions can be attributed to the different nature of the $2^1A'$ state: (HOMO-1) → LUMO for benzaldehyde and a pure minus state for styrene.

3.2.2. Singlet Rydberg States. Here we discuss the CASPT2 excitation energies and assignments for the states described by excitations out of the HOMO and n lone pair to the 3s and to the different components of the 3p and 3d Rydberg orbitals. Because of the close spacing between the HOMO − 1 and HOMO (see Figure 2), the corresponding members of Rydberg series converging to these two ionization potentials are expected to overlap in energy even for the early series members. For technical reasons, only the lowest π → Rydberg series have been explicitly computed. The low spatial symmetry of the molecule makes that too many roots are required to simultaneously obtain the full description of both π and π' Rydberg series. The second π' → Rydberg series are estimated to lie around 0.1−0.3 eV above the corresponding states of the π → Rydberg series. Anyway, as a byproduct of the computation, the $10^1A'(\pi' \rightarrow 3p_z)$ state has also been characterized (cf. Table 4).

The lowest Rydberg singlet state $2^1A''(\pi \rightarrow 3s)$ is computed at 6.54 eV, close to the shoulder observed at 6.67 eV on the high energy side of the most intense band of the vapor phase spectrum.[6] The $6^1A'(n \rightarrow 3s)$ state, obtained 7.03 eV above the ground state, could be related to the weak band observed at 6.97 eV that was initially assigned to 3*p* Rydberg transitions.[6,40] It is worth mentioning that the valence excited state $7^1A'$ is also placed in the same energy region. The spectroscopic study undertaken by Walsh in the high-energy region[4] revealed several rather diffuse bands ranging between 6.9 and 7.8 eV, being the strongest a doublet feature around 7.4 eV. It can be tentatively related to the $\pi \rightarrow 3p_z$ and $\pi' \rightarrow 3p_z$ Rydberg states, computed at 7.50 and 7.59 eV, mainly described by one-electron promotions coming out of the HOMO and HOMO − 1, respectively. In light of the theoretical spectrum, compiled in Table 4, the π → 3p and n → 3p Rydberg transitions can be associated with most of the diffuse features observed in this energy region. In addition, the valence excited state $9^1A'$ has been computed at 7.58 eV with a nonnegligible oscillator strength. It is, therefore, expected to contribute in the description of the bands observed in this energy region. The π → 3d and n → 3d states are predicted between 7.8 and 8.6 eV with small oscillator strengths. As far as we know, no experimental data are available to be compared with.

3.2.3. Lowest Triplet Valence States. Since many years ago, the characterization of the low-lying triplet states of benzaldehyde has been a major subject of investigation. However, up to date there is not a firm explanation to rationalize the efficient singlet−triplet intersystem crossing, which ultimately leads to phosphorescence. The relative ordering of the low-lying triplet states with respect to the lowest singlet excited-state $S_1(n\pi^*)$, assumed to be the most plausible candidate for a nonradiative transition to the triplet system, is a particularly relevant key issue.

The singlet−triplet spectrum computed at the ground-state optimal geometry places the lowest triplet state $T_1(n\pi^*)$ at 3.40 eV. The $n\pi^*$ character of the state is in agreement with experimental evidence.[11,15] The second triplet state $T_2(\pi\pi^*)$, computed at a slightly higher transition energy (3.49 eV), is mainly described by the HOMO → LUMO singly excited configuration. It is found to be 0.46 eV above the homologous triplet state of styrene, consistent with the larger HOMO−LUMO energy gap of benzaldehyde (see Figure 2). The singlet−triplet splitting is calculated to be 1.40 eV, somewhat smaller than the corresponding value determined for styrene (1.94 eV). The electron density differences of the triplet states relative to the ground state are shown in Figure 5.

The effects that relaxation within each of the triplet states brings on the remaining low-lying states can be inferred from the results obtained at different regions of the excited states complex hypersurfaces. By inspection of Table 3, it is easy to see that a dynamical interconversion between the $n\pi^*$and $\pi\pi^*$ triplet states may occur, as it has been indeed observed in spectroscopic studies of beam isolated benzaldehyde.[13] The spectroscopic techniques employed, such as vapor phosphorescence[14,15] or sensitized phosphorescence excitation,[11] place the 0−0 transition of $T_1(n\pi^*)$ and $T_2(\pi\pi^*)$ at 3.12 and 3.3 eV, in agreement with the theoretical values of 3.07 and 3.16 eV, respectively.

There is, however, a question that remains to be explained: the efficient mechanism for the S_1−T intersystem crossing. Experimental absorption studies place both triplet states below the lowest singlet excited-state $S_1(n\pi^*)$. Therefore, the important role of the environment to achieve an isoenergetic situation for

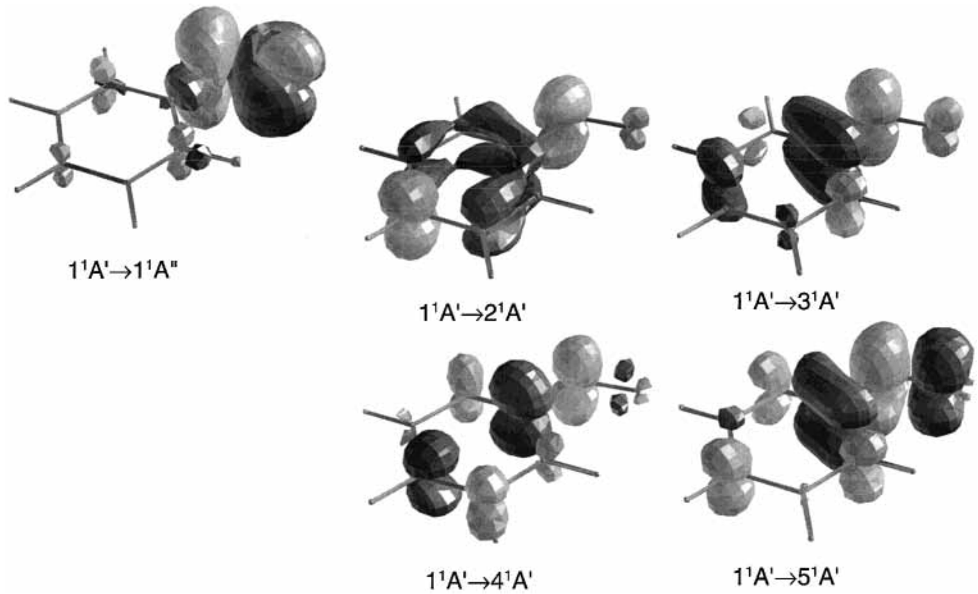

Figure 3. Differential electron density for the main singlet−singlet transitions in benzaldehyde. The electron density is shifted upon light-induced excitation from darker to lighter areas.

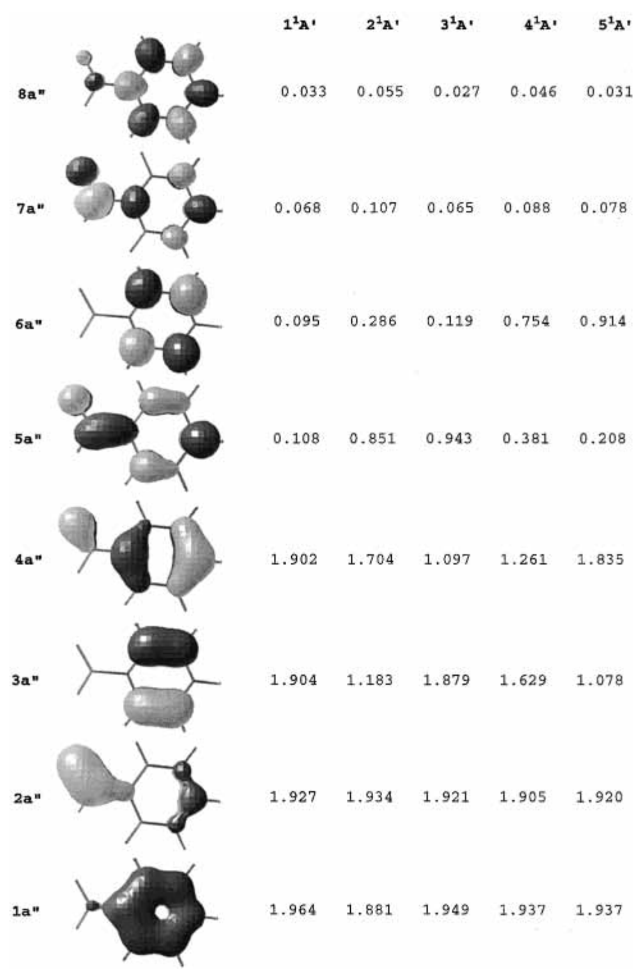

Figure 4. Occupation numbers of natural orbitals for the ground state and the low-lying $\pi\pi^*$ singlet excited states from the respective PMCAS-CI wave functions.

the $T_2(\pi\pi^*)$ and $S_1(n\pi^*)$ states, most plausible candidates for the singlet−triplet intersystem crossing, has been invoked.[11] Nevertheless, the mechanism is also efficient for isolated benzaldehyde. The two states follow the same scheme both

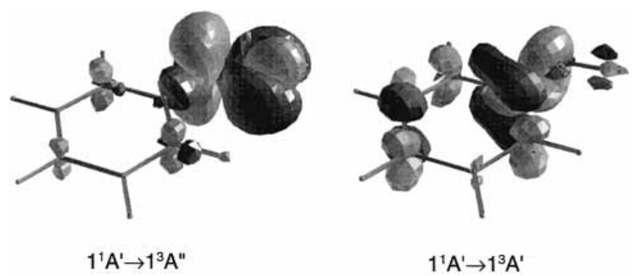

Figure 5. Differential electron density for the lowest singlet−triplet transitions in benzaldehyde. The electron density is shifted upon light-induced excitation from darker to lighter areas.

vertically and adiabatically in the current theoretical description. At the S_1 optimal geometry (see Table 3), the relative ordering between S_1 and T_2 is, however, reversed. It implies that the corresponding potential hypersurfaces intersect each other in the relaxation process of S_1, leading to a more favorable situation for the occurrence of an efficient intersystem crossing. Further investigation on the S_1−T_2 interstate coupling could provide crucial information for the conclusive establishment of the actual mechanism.

4. Summary and Conclusions

We have presented results from a fully correlated ab initio investigation of the electronic spectrum of benzaldehyde by means of using the MS-CASPT2 method, a well-established procedure for accurate calculations of electronic spectra of organic compounds.

Transitions to the singlet valence excited states are responsible of the experimental bands observed in the low-energy region of the electronic spectrum of benzaldehyde. The three lowest singlet excited states ($1^1A''$, $2^1A'$, and $3^1A'$) located at 3.71, 4.33, and 4.89 eV can be related to the maxima of the lowest-, second-, and third-energy absorption bands. Two electronic transitions with significant oscillator strength values are found in the energy range 5.9−6.3 eV. They correspond to the fourth-energy band of the one-photon absorption spectrum. The lowest triplet state of $n\pi^*$ character has been found at 3.40 eV, in agreement with the available experimental data from phosphorescence emission and sensitized phosphorescence excitation spectra. The second triplet state of $\pi\pi^*$ nature is computed at a slightly higher transition energy (3.49 eV).

The $\pi \rightarrow$ 3s and n $\rightarrow$ 3s Rydberg transitions are computed on the high-energy side of the most intense feature of the spectrum. The excited states corresponding to promotions to 3p-type Rydberg orbitals are related to the diffuse bands detected between 6.9 and 7.8 eV. We have tentatively assigned the intense doublet observed around 7.4 eV to the π, $\pi' \rightarrow 3p_z$ Rydberg states, computed at 7.50 and 7.59 eV, involving the nearly degenerate HOMO(π) and HOMO $-$ 1(π'), respectively. The Rydberg series to 3d diffuse orbitals are found at higher energies where no feature has been so far recorded. In addition, three valence excited states are predicted to be interleaved among the Rydberg states.

Geometry optimizations have been performed at the CASSCF level for the lowest singlet and triplet excited states of the $n\pi^*$ and $\pi\pi^*$ character. The singlet and triplet $n\pi^*$ states show similar relaxation trends. Upon optimization, the carbonyl bond is clearly elongated and the C_1-C_2 bond distance is shortened. The phenyl group develops a quinoid character when benzaldehyde relaxes in the triplet $\pi\pi^*$ state. On the other hand, optimization of the lowest $\pi\pi^*$ singlet state leads to a conformation with all of the aromatic bond distances increased by a mean value of 0.036 Å.

An attempt to rationalize the triplet manifold, ultimately leading to an intense phosphorescence, has also been performed. We have shown that the relative ordering of the lowest $n\pi^*$ and $\pi\pi^*$ triplet states changes depending on the geometry of the system. Relaxation in the lowest singlet state causes the intersection between the $S_1(n\pi^*)$ and $T_2(\pi\pi^*)$ potential hypersurfaces, that is, an optimal situation for an efficient intersystem crossing.

Acknowledgment. The research reported in this paper has been supported by the DGES project No. PB97-1377 of Spain, the European Commission TMR network Contract ERB FMRX-CT96-0079 (Quantum Chemistry for the Excited State), and the *Generalitat Valenciana*. V.M. thanks the *Generalitat Valenciana* for a personal grant.

References and Notes

(1) Molina, V.; Smith, B. R.; Merchán, M. *Chem. Phys. Lett.* **1999**, *309*, 486.

(2) Molina, V.; Merchán, M.; Malmqvist, P.-Å.; Roos, B. O. *Phys. Chem. Chem. Phys.* **2000**, *2*, 2211.

(3) Silva, C. R.; Reilly, J. P. *J. Phys. Chem.* **1996**, *100*, 17111.

(4) Walsh, A. D. *Trans. Faraday Soc.* **1946**, *42*, 62.

(5) Walsh, A. D. *Proc. R. Soc. (London)* **1947**, *A 191*, 32.

(6) Kimura, K.; Nagakura, S. *Theor. Chim. Acta* **1965**, *3*, 164.

(7) Abe, H.; Kamei, S.; Mikami, N.; Ito, M. *Chem. Phys. Lett.* **1984**, *109*, 217.

(8) Smolarek, J.; Zwarich, R.; Goodman, L. *J. Mol. Spectrosc.* **1972**, *43*, 416.

(9) Berger, M.; Goldblatt, I. L.; Steel, C. *J. Am. Chem. Soc.* **1973**, *95*, 1717.

(10) Leopold, D. G.; Hemley, R. J.; Vaida, V.; Roebber, J. L. *J. Chem. Phys.* **1981**, *75*, 4758.

(11) Ohmori, N.; Suzuki, T.; Ito, M. *J. Phys. Chem.* **1988**, *92*, 1086.

(12) Villa, E.; Amirav, A.; Chen, W.; Lim, E. C. *Chem. Phys. Lett.* **1988**, *147*, 43.

(13) Sneh, O.; Cheshnovsky, O. *J. Phys. Chem.* **1991**, *95*, 7154.

(14) Goodman, L.; Koyanagi, M. *Mol. Photochem.* **1972**, *4*, 369.

(15) Koyanagi, M.; Goodman, L. *Chem. Phys.* **1979**, *39*, 237.

(16) Hollas, J. M.; Thakur, S. N. *Chem. Phys.* **1973**, *1*, 385.

(17) Inuzuka, K.; Yokota, T. *Bull. Chem. Soc. Jpn.* **1965**, *38*, 1055.

(18) Ridley, J. E.; Zerner, M. C. *J. Mol. Spectrosc.* **1979**, *76*, 71.

(19) Andersson, K.; Malmqvist, P.-Å.; Roos, B. O.; Sadlej, A. J.; Wolinski, K. *J. Phys. Chem.* **1990**, *94*, 5483.

(20) Andersson, K.; Malmqvist, P.-Å.; Roos, B. O. *J. Chem. Phys.* **1992**, *96*, 1218.

(21) Finley, J.; Malmqvist, P.-Å.; Roos, B. O.; Serrano-Andrés, L. *Chem. Phys. Lett.* **1998**, *288*, 299.

(22) Roos, B. O.; Fülscher, M. P.; Malmqvist, P.-Å.; Merchán, M.; Serrano-Andrés, L. In *Quantum Mechanical Electronic Structure Calculations with Chemical Accuracy*; Langhoff, S. R., Ed.; Kluwer Academic Publishers: Dordrecht, The Netherlands, 1995; p 357.

(23) Roos, B. O.; Andersson, K.; Fülscher, M. P.; Malmqvist, P.-Å.; Serrano-Andrés, L.; Pierloot, K.; Merchán, M. In *Advances in Chemical Physics: New Methods in Computational Quantum Mechanics*; Prigogine, I., Rice, S. A., Eds.; John Wiley & Sons: New York, 1996; Vol. XCIII, p 219.

(24) Merchán, M.; Serrano-Andrés, L.; Fülscher, M. P.; Roos, B. O. In *Recent Advances in Multireference Methods*; K. H. U., Ed.; World Scientific Publishing Co.: Singapore, 1999; Vol. IV, p 161.

(25) Widmark, P.-O.; Malmqvist, P.-Å.; Roos, B. O. *Theor. Chim. Acta* **1990**, *77*, 291.

(26) Rubio, M.; Merchán, M.; Ortí, E.; Roos, B. O. *Chem. Phys.* **1994**, *179*, 395.

(27) Rubio, M.; Merchán, M.; Ortí, E.; Roos, B. O. *Chem. Phys. Lett.* **1995**, *234*, 373.

(28) Molina, V.; Merchán, M.; Roos, B. O. *J. Phys. Chem. A* **1997**, *101*, 3478.

(29) Molina, V.; Merchán, M.; Roos, B. O. *Spectrochim. Acta* **1999**, *55A*, 433.

(30) Proppe, B.; Merchán, M.; Serrano-Andrés, L. *J. Phys. Chem. A* **2000**, *104*, 1608.

(31) Malmqvist, P.-Å. *Int. J. Quantum Chem.* **1986**, *30*, 479.

(32) Malmqvist, P.-Å.; Roos, B. O. *Chem. Phys. Lett.* **1989**, *155*, 189.

(33) Andersson, K.; Blomberg, M. R. A.; Fülscher, M. P.; Karlstöm, G.; Lindh, R.; Malmqvist, P.-Å.; Neogrády, P.; Olsen, J.; Roos, B. O.; Sadlej, A. J.; Schütz, M.; Seijo, L.; Serrano-Andrés, L.; Siegbahn, P. E. M.; Widmark, P.-O. *MOLCAS*, version 4.0; University of Lund: Lund, Sweden, 1997.

(34) Borisenko, K. B.; Bock, C. W.; Hargittai, I. *J. Phys. Chem.* **1996**, *100*, 7426.

(35) Merchán, M.; Roos, B. O. *Theor. Chim. Acta* **1995**, *92*, 227.

(36) Merchán, M.; Roos, B. O.; McDiarmid, R.; Xing, X. *J. Chem. Phys.* **1996**, *104*, 1791.

(37) Pou-Amérigo, R.; Merchán, M.; Ortí, E. *J. Chem. Phys.* **1999**, *110*, 9536.

(38) Herzberg, G. *Molecular Spectra and Molecular Structure*; Krieger Publishing Company: Malabar, FL 1991; Vol. III.

(39) Oumi, M.; Maurice, D.; Lee, T. J.; Head-Gordon, M. *Chem. Phys. Lett.* **1997**, *279*, 151.

(40) Robin, M. B. *Higher Excited States of Polyatomic Molecules*; Academic Press: New York, 1975; Vol. II.